



ELSEVIER

26 October 2000

PHYSICS LETTERS B

Physics Letters B 492 (2000) 56–62

www.elsevier.nl/locate/npe

Effect of the charm quark mass on the BFKL $\gamma^*\gamma^*$ total cross section at LEP[☆]

Jochen Bartels^{a,*}, Carlo Ewerz^{b,c}, René Staritzbichler^a^a *Institut für Theoretische Physik, Universität Hamburg, Luruper Chaussee 149, D-22761 Hamburg, Germany*^b *Cavendish Laboratory, Cambridge University, Madingley Road, Cambridge CB3 0HE, UK*^c *DAMTP, Centre for Mathematical Sciences, Cambridge University, Wilberforce Road, Cambridge CB3 0WA, UK*

Received 10 April 2000; received in revised form 6 September 2000; accepted 25 September 2000

Editor: P.V. Landshoff

Abstract

We perform a numerical study of various improvements of the LO BFKL prediction for the $\gamma^*\gamma^*$ total cross section in the kinematical region of the L3 detector at LEP. In particular, we study the effects of a massive charm quark and of different photon polarizations. The variation of the BFKL prediction under changes of α_s is investigated. © 2000 Elsevier Science B.V. All rights reserved.

1. Introduction

The total hadronic cross section in $\gamma^*\gamma^*$ scattering at electron–positron colliders is considered to be a suitable observable for studying the interesting dynamics of QCD at small x . For sufficiently large photon virtualities one expects this process to be the optimal test of the perturbative (BFKL) Pomeron [1]. The process is being studied by the L3 and the OPAL collaborations [2,3] at LEP. First analytic calculations based upon the leading order (LO) BFKL approximation [4,5] have been compared to measurements by the

L3 collaboration [2]. In the meantime various aspects of this process have been considered in more detail [6–13]. In summary, the present situation is similar to that of forward jets at HERA [14]. The data points for the total $\gamma^*\gamma^*$ cross section lie above the two-gluon exchange approximation but clearly below the LO BFKL prediction. First attempts to include the NLO corrections [15,16] (see also [17]) to the BFKL approximation are encouraging [11,13] but not yet conclusive: for a consistent NLO calculation of the $\gamma^*\gamma^*$ cross section one needs the NLO corrections to the photon impact factors which have not yet been calculated. Also the NLO corrections to the two-gluon exchange approximation need to be calculated before final conclusions can be drawn.

But even the LO calculations still suffer from several theoretical uncertainties which we would like to discuss in this short note. Previous calculations of the $\gamma^*\gamma^*$ cross section have been performed for massless quarks only, and the L3 data have been

[☆] Work supported in part by the EU Fourth Framework Programme “Training and Mobility of Researchers”, Network “Quantum Chromodynamics and the Deep Structure of Elementary Particles”, contract FMRX-CT98-0194 (DG 12-MIHT).

* Corresponding author.

E-mail addresses: bartels@x4u2.desy.de (J. Bartels), carlo@hep.phy.cam.ac.uk (C. Ewerz), staritz@mail.desy.de (R. Staritzbichler).

compared to the prediction for four massless quarks. In the kinematic range of LEP, however, the charm mass is not negligible. The correct cross section lies between the ones for three and four massless quarks. But due to the charge $+2/3$ of the charm quark the cross section is multiplied by a factor of 2.8 when going from three to four massless flavors. Thus it is obviously very desirable to determine the effect of the charm quark mass more precisely. Effects of the charm mass have so far only been considered in [11] where a formula was given in x -space and its effect was not considered separately. We give a formula for the cross section for non-zero charm quark mass in Mellin space and perform a numerical study which shows that the charm quark mass leads to a considerable reduction of the cross section expected for LEP. The theoretical prediction of the cross section also depends on the value of the strong coupling constant α_s which is not too well known at the (comparatively small) momentum scales dominating the kinematics at LEP, especially at $\sqrt{s} = 91$ GeV. Our numerical study shows that the dependence on α_s is rather strong. Further, we briefly discuss the effect of taking into account contributions from all photon polarizations as well as the uncertainty associated with the BFKL energy scale.

2. Cross section formula

In the events of interest the scattered electron as well as the scattered positron are tagged ('double-tag events'), and we define useful scaling variables (we use the notation of [4])

$$x_1 = \frac{Q_1^2}{2q_1k_2}, \quad x_2 = \frac{Q_2^2}{2q_2k_1} \quad (1)$$

and

$$y_1 = \frac{q_1k_2}{k_1k_2}, \quad y_2 = \frac{q_2k_1}{k_1k_2}, \quad (2)$$

where k_1 and k_2 are the momenta of the electron and positron, respectively. We have

$$y_i = 1 - \frac{E_{\text{tag}}^i}{E_b} \cos^2\left(\frac{\theta_{\text{tag}}^i}{2}\right), \quad (3)$$

where E_b is the beam energy, and E_{tag}^i and θ_{tag}^i are the energy of the tagged lepton and its angle with respect

to the beam axis, respectively. The virtualities of the photons are ($i = 1, 2$)

$$Q_i^2 = -q_i^2 = 2E_b E_{\text{tag}}^i (1 - \cos\theta_{\text{tag}}^i), \quad (4)$$

and they are required to be large to make perturbation theory applicable. The squared center-of-mass energy of the e^+e^- collisions is $s = (k_1 + k_2)^2$, whereas for the underlying $\gamma^*\gamma^*$ process the squared energy is given by

$$\hat{s} = (q_1 + q_2)^2 \simeq sy_1y_2. \quad (5)$$

We consider the limit where Q_1^2, Q_2^2 and \hat{s} are large and

$$Q_1^2, Q_2^2 \ll \hat{s}. \quad (6)$$

The differential e^+e^- cross section has been calculated in [4] and [5]. The total $\gamma^*\gamma^*$ cross section is given by

$$\sigma_{\gamma^*\gamma^*} = \sigma_{\gamma^*\gamma^*}^{TT} + \epsilon_2\sigma_{\gamma^*\gamma^*}^{TL} + \epsilon_1\sigma_{\gamma^*\gamma^*}^{LT} + \epsilon_1\epsilon_2\sigma_{\gamma^*\gamma^*}^{LL} \quad (7)$$

with

$$\epsilon_i = \frac{2(1 - y_i)}{1 + (1 - y_i)^2}. \quad (8)$$

The labels T and L refer to the transverse and longitudinal polarization of the incoming photon, respectively. In [2] it has been argued that in the L3 region the ϵ_i have values larger than 0.97. For simplicity we take them as 1 which leads to a deviation of less than 3 percent. For the polarizations $i, j \in \{L, T\}$ of the initial photons one finds

$$\begin{aligned} \sigma_{\gamma^*\gamma^*}^{ij} &= \frac{\alpha_{\text{em}}}{16Q_1^2} \frac{\alpha_{\text{em}}}{16Q_2^2} \int \frac{dv}{2\pi^2} \exp\left[\ln\left(\frac{\hat{s}}{s_0}\right)\chi(v)\right] \\ &\quad \times W_i\left(v, \frac{m^2}{Q_1^2}\right) W_j\left(-v, \frac{m^2}{Q_2^2}\right), \end{aligned} \quad (9)$$

where s_0 is the typical BFKL energy scale which we choose as

$$s_0 = \sqrt{Q_1^2 Q_2^2}. \quad (10)$$

Further,

$$\chi(v) = \frac{N_c\alpha_s}{\pi[2\psi(1) - \psi(1/2 + iv) - \psi(1/2 - iv)]}, \quad (11)$$

and ψ denotes the digamma function. For massless quarks the functions W_i are given in [4]. For massive quarks we can use the results found in [18] to obtain

$$\begin{aligned}
W_L\left(v, \frac{m_c^2}{Q_i^2}\right) &= \sum_{f=u,d,s} 8\sqrt{2}q_f^2\alpha_s\pi^2 \frac{v^2 + \frac{1}{4}}{v^2 + 1} \frac{\sinh \pi v}{v \cosh^2 \pi v} (Q_i^2)^{\frac{1}{2}+iv} \\
&+ \frac{128}{15}\sqrt{2}q_c^2\alpha_s\pi\sqrt{\pi} \frac{\Gamma(\frac{3}{2} + iv)}{\Gamma(2 + iv) \cosh \pi v} \\
&\times (Q_i^2)^{\frac{1}{2}+iv} \left(\frac{Q_i^2 + 4m_c^2}{Q_i^2}\right)^{-\frac{3}{2}-iv} \\
&\times {}_2F_1\left(\frac{3}{2} + iv, \frac{1}{2}; \frac{7}{2}; \frac{Q_i^2}{Q_i^2 + 4m_c^2}\right) \quad (12)
\end{aligned}$$

and

$$\begin{aligned}
W_T\left(v, \frac{m_c^2}{Q_i^2}\right) &= \sum_{f=u,d,s} 4\sqrt{2}q_f^2\alpha_s\pi^2 \frac{v^2 + \frac{9}{4}}{v^2 + 1} \frac{\sinh \pi v}{v \cosh^2 \pi v} (Q_i^2)^{\frac{1}{2}+iv} \\
&+ 16\sqrt{2}q_c^2\alpha_s\pi\sqrt{\pi} \frac{\Gamma(\frac{1}{2} + iv)}{\Gamma(2 + iv) \cosh \pi v} \\
&\times (Q_i^2)^{\frac{1}{2}+iv} \left(\frac{Q_i^2 + 4m_c^2}{Q_i^2}\right)^{\frac{1}{2}-iv} \\
&\times \left\{ \left[\frac{(1 + 3iv)Q_i^2 + (3 + 2iv)m_c^2}{Q_i^2 + 4m_c^2} \right. \right. \\
&\quad \left. \left. - iv \left(\frac{Q_i^2}{Q_i^2 + 4m_c^2}\right)^2 \right] \right. \\
&\times {}_2F_1\left(\frac{1}{2} + iv, \frac{1}{2}; \frac{3}{2}; \frac{Q_i^2}{Q_i^2 + 4m_c^2}\right) \\
&+ \left[(1 - iv) \frac{Q_i^2}{Q_i^2 + 4m_c^2} - \frac{3 + 2iv}{4} \right] \\
&\left. \times {}_2F_1\left(-\frac{1}{2} + iv, \frac{1}{2}; \frac{3}{2}; \frac{Q_i^2}{Q_i^2 + 4m_c^2}\right) \right\}, \quad (13)
\end{aligned}$$

where q_f denotes the electric charge of the quark flavor f . The terms containing $q_c = 2/3$ correspond to the contribution of the charm quark. In the limit $m_c \rightarrow 0$ they can be simplified in such a way that the sum over flavours in the first terms is extended to include four flavours. The bottom quark — relevant to experiments at a future Linear Collider — can be included in the same way as the charm quark. (The

contribution of the bottom quark is very small at LEP and will be neglected in the following.)

3. Numerical results

For our numerical analysis we use the kinematics of the L3 detector (see also [2]). At LEP91 the outgoing electrons close to the forward direction can be detected within the angles $30 \text{ mrad} < \theta_{\text{tag}} < 66 \text{ mrad}$, and the electron energy required for tagging is $E_{\text{tag}} > 30 \text{ GeV}$. This leads to a range of possible photon virtualities

$$1.2 \text{ GeV}^2 < Q_{1,2}^2 < 9 \text{ GeV}^2, \quad (14)$$

and the cross section is evaluated at the mean value $\langle Q^2 \rangle = 3.5 \text{ GeV}^2$.

At LEP183 the energy of the tagged electrons is restricted by $E_{\text{tag}} > 40 \text{ GeV}$, and the angular range is the same as at LEP91. The virtualities are

$$2.5 \text{ GeV}^2 < Q_{1,2}^2 < 35 \text{ GeV}^2, \quad (15)$$

with the mean value $\langle Q^2 \rangle = 14 \text{ GeV}^2$. Note that with these mean values of Q^2 the available range for the rapidity $Y = \ln(\hat{s}/s_0)$ is the same for LEP91 and LEP183.

In the BFKL formalism the strong coupling α_s is kept fixed, and the natural scale is $\langle Q^2 \rangle$. In our numerical study we therefore use different values of α_s for different virtualities $\langle Q^2 \rangle$. Specifically, we determine α_s from the given virtuality using a running α_s in NNLO with four active flavours. One should keep in mind that the experimental data cover a range of virtualities with $\langle Q^2 \rangle$ being the mean values. Therefore the correct choice of α_s is not obvious. We study a range of values of α_s , the variation of α_s used for a given scale $\langle Q^2 \rangle$ (see below) is obtained by varying Λ_{QCD} (approximately between 100 MeV and 350 MeV).

The results of our numerical study are illustrated in the following figures. Fig. 1 shows a comparison between the saddle point approximation to the BFKL cross section and the exact calculation of the LO BFKL Pomeron, here for LEP183 and for transversely polarized photons only. In order to allow for a direct comparison with the theoretical curve used in [2], the curves in this and in the next figure are calculated for four massless quarks (mass effects are discussed

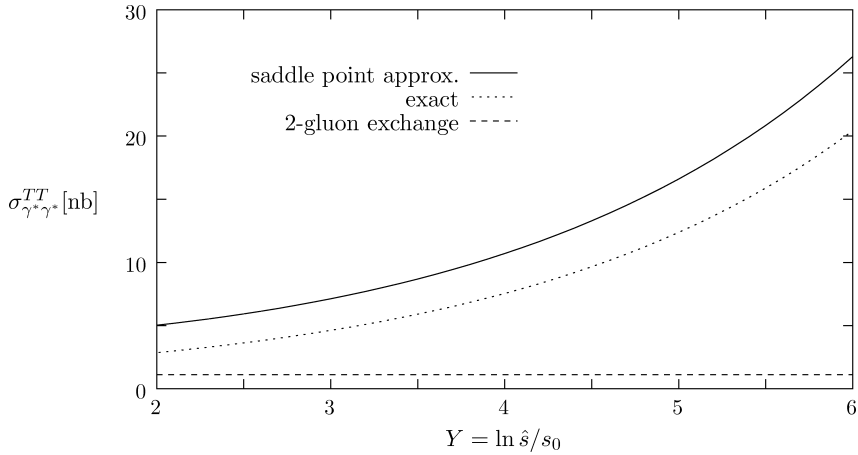


Fig. 1. Comparison of the exact BFKL result with the saddle point approximation and the two-gluon exchange approximation for transversely polarized photons at LEP183 with $\langle Q^2 \rangle = 14 \text{ GeV}^2$, $\alpha_s = 0.208$.

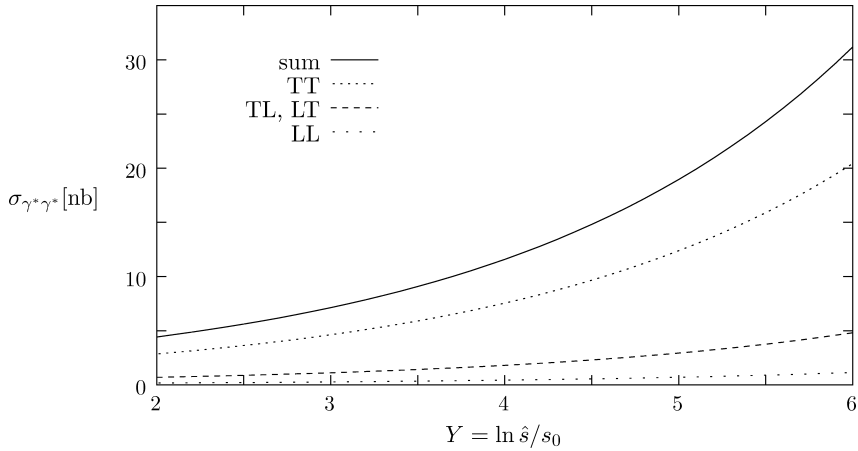


Fig. 2. Contributions of different photon polarizations to the cross section, here for LEP 183 with $\langle Q^2 \rangle = 14 \text{ GeV}^2$, $\alpha_s = 0.208$, $m_c = 0$.

separately below). In [2] the measured data have been compared to the saddle point approximation. We find that this approximation overestimates the exact cross section by 20% to 30%. Fig. 1 also shows the cross section obtained from two-gluon exchange which approximates the full DGLAP formalism if the two photon virtualities are of the same order.

Next we show in Fig. 2 the contributions of different polarizations of the two incoming photons, again for LEP183 and with four massless quarks. Clearly the sum of all polarization is substantially larger than

the transverse contribution alone which was compared with data in [2].

Now we address the question how the cross section depends on the value of α_s chosen at the scale $\langle Q^2 \rangle$. Here and in the following we include the charm quark as a massive quark and sum over all photon polarizations, i.e., we use Eq. (7) with Eqs. (9), (12), (13). As can be seen from Eqs. (9) and (11), α_s enters in the exponent and thus we expect a strong dependence of the cross section on its particular value. This is confirmed by the numerical results presented in Figs. 3 and 4. Fig. 3 shows the cross section for

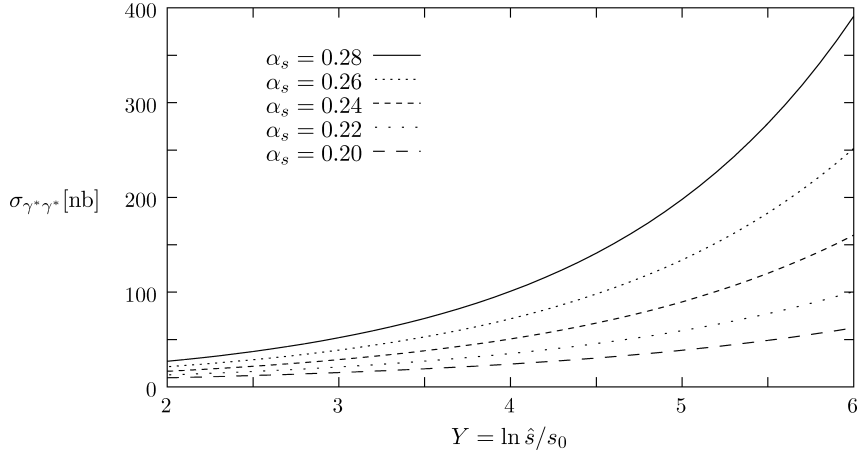


Fig. 3. Energy dependence of the $\gamma^*\gamma^*$ cross section for different values of α_s ($\langle Q^2 \rangle$), here for LEP91 with $\langle Q^2 \rangle = 3.5 \text{ GeV}^2$, $m_c = 1.5 \text{ GeV}$.

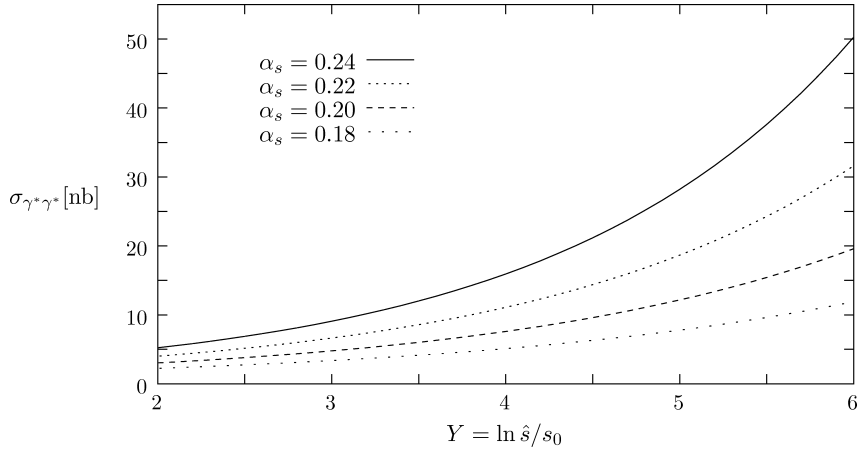


Fig. 4. Same as Fig. 3, here for LEP183 with $\langle Q^2 \rangle = 14 \text{ GeV}^2$.

$\langle Q^2 \rangle = 3.5 \text{ GeV}^2$ (LEP91), and we study a spread $0.20 < \alpha_s < 0.28$ of possible values. In Fig. 3 we have plotted the cross section for $\langle Q^2 \rangle = 14 \text{ GeV}^2$ (LEP183), now varying α_s between 0.18 and 0.24. In [2] the theoretical curves were obtained using $\alpha_s = 0.20$ for both energies. For LEP91 this choice appears very low. To obtain more realistic predictions (see below), we choose $\alpha_s = 0.268$ (LEP91) and $\alpha_s = 0.208$ (LEP183), respectively.

A further uncertainty is the choice of the BFKL energy scale s_0 . Strictly speaking, its value is not determined in the leading order BFKL formalism. In this sense, the choice (10) is only an educated guess.

It is well possible that the true value differs from that choice by a factor of two, for example. Choosing s_0 as twice (half) the value given in (10) results in a shift of the BFKL prediction to the right (left) by $\ln 2 \simeq 0.7$ units in rapidity. Shifting the curves in our figures by this value amounts to a considerable change in the LO BFKL prediction. However, the uncertainty in s_0 is less serious in the NLO BFKL calculation since there the typical curves are less steep and a horizontal shift results in a smaller absolute change of the cross section.

Finally, we study the effect of the charm quark mass on the cross section. Our results (including also the

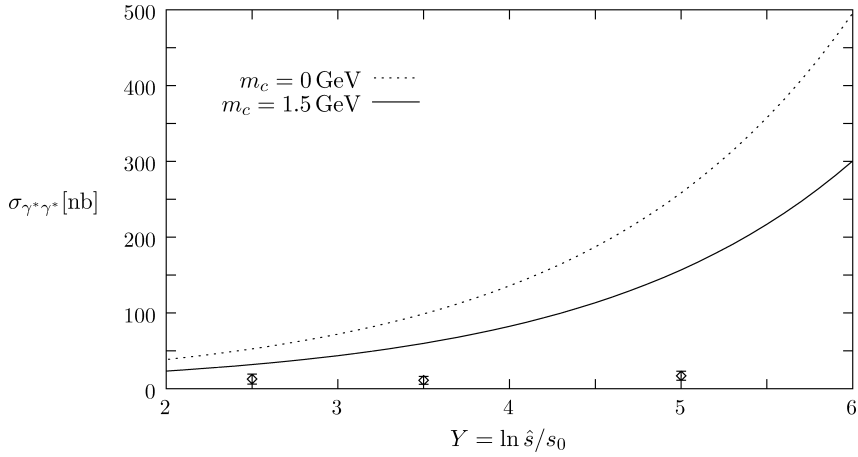


Fig. 5. Effect of the charm quark mass on the $\gamma^*\gamma^*$ cross section for LEP 91 with $\langle Q_i^2 \rangle = 3.5 \text{ GeV}^2$, $\alpha_s = 0.268$. Data points as measured by the L3 Collaboration [2].

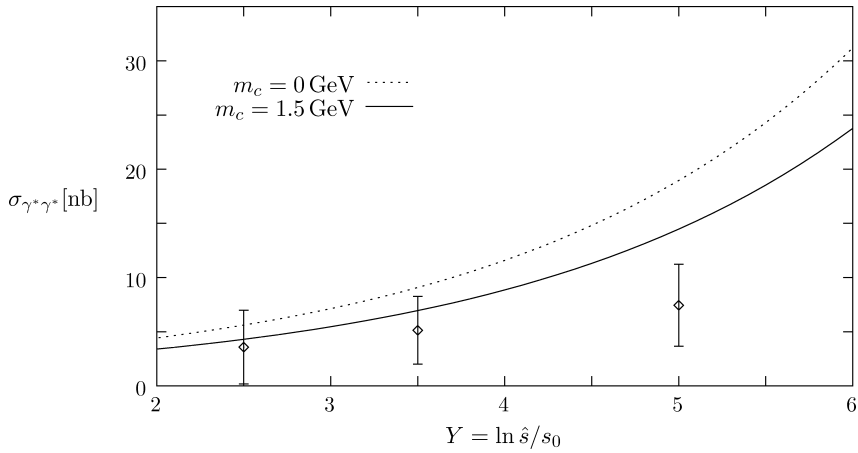


Fig. 6. Same as Fig. 5, here for LEP183 with $\langle Q^2 \rangle = 14 \text{ GeV}^2$, $\alpha_s = 0.208$.

improvements discussed above) are shown in Fig. 5 for LEP91, and in Fig. 6 for LEP183. For LEP91 the charm quark mass reduces the cross section by about 30% (compared to a massless charm quark), for LEP183 the cross section is reduced by about 20%. The effect of the charm mass is different in the two cases due to the different mean values $\langle Q^2 \rangle$. It can be seen immediately from Eqs. (12) and (13) that the charm mass m_c enters in such a combination with Q^2 that for increasing Q^2 the effect of a finite m_c becomes weaker. Also shown in Figs. 5 and 6 are the data points measured by the L3 collaboration [2]. One should note

that in these data the contribution of the quark box diagram — or quark parton model (QPM) graph — has already been subtracted. This diagram is also not included in our calculation.

Compared with the theoretical prediction used in [2] we have made the following changes to arrive at the cross sections in Figs. 5 and 6: exact BFKL is used instead of the saddle point approximation, all photon polarizations are included, and a nonzero charm quark mass is used. Further we have chosen a higher (and more realistic) value for α_s in the case of LEP91. Roughly speaking, the first three changes lead

to a change in the normalization, whereas the last one results in a different energy dependence. For LEP91 we find a significantly larger cross section than the one given by the theoretical curve in [2]. Here the main effect is due to the choice of α_s . For LEP183 our prediction is very close to the one used in [2] because the changes almost compensate each other. However, one should have in mind that already a small change in α_s leads to a visible modification of the energy dependence.

Our predictions for the cross section are higher and exhibit a much faster rise with energy than the measured data points (especially in the case of LEP91). This was to be expected since the NLO corrections to the BFKL equation are known to be sizable and lead to a slower rise with energy. Certainly there is a good chance to successfully describe the data by a NLO BFKL calculation. However, also there one should keep in mind the uncertainties discussed above.

4. Conclusions

Our study of the BFKL prediction shows that the approximations made in previous analyses are numerically significant. Moreover, there are substantial theoretical uncertainties at the LO level due to the uncertainty in the choice of α_s . However, also an improved treatment does not change the main conclusion: the LEP data for the total hadronic $\gamma^*\gamma^*$ cross section clearly indicate that a simple two-gluon exchange is not sufficient to describe the data. The LO BFKL prediction, on the other hand, lies well above the data. A consistent NLO calculation including the impact factors is therefore urgently needed.

Acknowledgements

CE would like to thank G. Salam, M. Wadhwa and M. Wüsthoff for helpful discussions.

References

- [1] E.A. Kuraev, L.N. Lipatov, V.S. Fadin, Sov. Phys. JETP 45 (1977) 199; Sov. J. Nucl. Phys. 28 (1978) 822.
- [2] L3 Collaboration, M. Acciarri et al., Phys. Lett. B 453 (1999) 333.
- [3] M. Przybycień, for the OPAL Collaboration, Nucl. Phys. B Proc. Suppl. 82 (2000) 67.
- [4] J. Bartels, A. De Roeck, H. Lotter, Phys. Lett. B 389 (1996) 742, hep-ph/9608401; J. Bartels, A. De Roeck, C. Ewerz, H. Lotter, hep-ph/9710500, in: R. Settles (Ed.), ECFA/DESY Study on Physics and Detectors for a Linear Collider, DESY 97-123E.
- [5] S.J. Brodsky, F. Hautmann, D.E. Soper, Phys. Rev. Lett. 78 (1997) 803; S.J. Brodsky, F. Hautmann, D.E. Soper, Phys. Rev. Lett. 79 (1997) 3522, hep-ph/9610260 (Erratum); S.J. Brodsky, F. Hautmann, D.E. Soper, Phys. Rev. D 56 (1997) 6957, hep-ph/9706427.
- [6] M. Boonekamp, A. De Roeck, C. Royon, S. Wallon, Nucl. Phys. B 555 (1999) 540, hep-ph/9812523.
- [7] A. Bialas, W. Czyz, W. Florkowski, Eur. Phys. J. C 2 (1998) 683, hep-ph/9705470.
- [8] N.N. Nikolaev, J. Speth, V.R. Zoller, hep-ph/0001120.
- [9] E. Gotsman, E. Levin, U. Maor, E. Naftali, hep-ph/0001080.
- [10] A. Donnachie, H.G. Dosch, M. Rueter, Eur. Phys. J. C 13 (2000) 141, hep-ph/9908413.
- [11] J. Kwieciński, L. Motyka, Phys. Lett. B 462 (1999) 203, hep-ph/9905567.
- [12] A. Donnachie, S. Söldner-Rembold, hep-ph/0001035, Proceedings of UK Phenomenology Workshop on Collider Physics, Durham 1999, in press.
- [13] S.J. Brodsky, V.S. Fadin, V.T. Kim, L.N. Lipatov, G.B. Pivovarov, JETP Lett. 70 (1999) 155, hep-ph/9901229.
- [14] H1 Collaboration, C. Adloff et al., Nucl. Phys. B 538 (1999) 3, hep-ex/9809028; ZEUS Collaboration, J. Breitweg et al., Eur. Phys. J. C 6 (1999) 239, hep-ex/9805016.
- [15] V.S. Fadin, L.N. Lipatov, Phys. Lett. B 429 (1998) 127, hep-ph/9802290, and references therein.
- [16] M. Ciafaloni, G. Camici, Phys. Lett. B 430 (1998) 349, hep-ph/9803389, and references therein.
- [17] M. Ciafaloni, D. Colferai, G.P. Salam, Phys. Rev. D 60 (1999) 114036, hep-ph/9905566.
- [18] K. Golec-Biernat, M. Wüsthoff, Phys. Rev. D 59 (1999) 014017, hep-ph/9807513.